

Minimizing Transmission Electron Microscopy Beam Damage during the Study of Surface Reactions on Sodium Chloride

Heather C. Allen,¹ Martha L. Mecartney,² and John C. Hemminger^{1*}

¹Department of Chemistry, University of California, Irvine, CA 92697

²Department of Chemical and Biochemical Engineering and Materials Science, University of California, Irvine, Irvine, CA 92697

Abstract: Electron beam damage is a significant limitation for transmission electron microscopy (TEM) studies of beam-sensitive samples. An approach for studying surface reactions on alkali halide crystals using 200 kV TEM is presented. Experiments were designed to monitor the reaction of NaCl crystals with HNO₃ gas followed by water vapor to form solid NaNO₃. During beam damage experiments, TEM micrographs record structural changes to both NaCl and NaNO₃, including dislocation loops, void formation, and decomposition. Sample decomposition can be successfully minimized by a combination of commonly used techniques: (1) focusing the beam adjacent to the area of interest, (2) lowering the electron density, (3) choosing to image larger (micrometer- versus submicrometer-sized) alkali halide crystals, and (4) lowering temperature by the use of a liquid nitrogen cooling stage. From these results, additional studies were designed that monitored sequential experiments. Sensitive micrometer-sized sodium chloride single crystals before and after exposure to nitric acid vapor and water vapor and the subsequent growth of submicrometer-sized sodium nitrate single crystals could then be successfully imaged using TEM.

Key words: NaCl, NaNO₃, HNO₃, water vapor, TEM, electron beam damage

INTRODUCTION

Sodium chloride is the dominant constituent of sea salt particles collected in the marine troposphere. There is an estimated flux of 10¹²–10¹³ kg of sea salt particles produced annually from wave action (Blanchard, 1985). Sea salt may be an important source of chlorine if sea salt reacts with nitrogen oxides to produce significant amounts of gas-

phase chlorine. In urban areas, pollutants produced from automobile exhaust (i.e., nitrogen oxides) react with sea salt particles which have been transported inland by local meteorological conditions (Sheridan et al., 1992; Shaw, 1991; DeBock et al., 1994; Hidy et al., 1974; Martens et al., 1973; Xhoffer et al., 1991). The reaction of sodium chloride with nitrogen oxides is important to study because of the negative implications that gas-phase chlorine products may have on atmospheric chemistry (i.e., ozone levels) (Finlayson-Pitts, 1993; Finlayson-Pitts and Pitts, 1986). One relevant reaction is:



Received May 27, 1997; accepted December 16, 1997.

Heather C. Allen is now at Department of Chemistry, University of Oregon, Eugene, OR 97403.

*Corresponding author

which produces sodium nitrate and gas-phase hydrogen chloride. Hydrogen chloride can combine with water in the atmosphere or in other ways react to form chlorine atoms (Graedel and Keene, 1995). Ultimately, through a series of reactions, chlorine atoms in the lower atmosphere may raise ozone levels (a component of smog).

The important hypotheses to investigate are: (1) whether the entire volume of sodium chloride crystals is available for reaction, or (2) does the nitrate formed passivate the surface of sodium chloride crystals, rendering the bulk of the sodium chloride inaccessible for further reaction? If only the sea salt's surface is available for reaction, substantially less chlorine will be emitted into the atmosphere, compared with the entire volume available. Therefore, it is important to find experimentally which hypothesis is correct to determine if sea salt particles could be a significant source of atmospheric gas-phase chlorine.

The reaction in equation (1) was used as a model system for TEM studies of the reaction of HNO_3 with NaCl crystals. Electron beam damage studies were conducted to establish experimental parameters to allow the successful observation of the sodium chloride reaction after exposure to nitric acid vapor and water vapor.

Several researchers have been conducting experiments on the reactions of sodium chloride with nitrogen oxides using other techniques such as diffuse reflectance Fourier Transform infrared spectroscopy, Knudsen cell studies, X-ray photoelectron spectroscopy, and flow reactors (Finlayson-Pitts 1983; Vogt et al., 1994a, 1994b; Leu et al., 1995; Laux et al., 1994, 1996; Fenter et al., 1994; Karlsson and Ljungstrom, 1995). Although these techniques have provided significant insight to the reaction mechanisms of NaCl with nitrogen oxides, there still exist unanswered questions (e.g., bulk versus surface availability). Complementary to these studies, microscopy techniques such as TEM offer visual identification and phase information (using electron diffraction) in addition to compositional analyses using energy dispersive spectroscopy (EDS).

Although TEM with EDS is an excellent analytical tool, there are limitations associated with using electron microscopies for imaging electron beam-sensitive materials. Posfai et al. (1995) have observed electron beam damage occurring while imaging atmospheric particulate matter. Huang and Turpin (1996) had significant problems with sulfate sublimation during electron beam exposures. There have been a number of studies that clearly demonstrate the fragility of alkali halides during electron irradiation. Previous TEM studies of sodium chloride have shown electron beam dam-

age as evidenced by dislocations and voids (Hobbs et al., 1993; Hobbs, 1974, 1976, 1979; Hibi and Yada, 1962).

With the above-stated difficulties, the use of TEM to follow a reaction sequence might be considered unreasonable. However, as shown here, a reaction sequence can be studied successfully. Posfai et al. (1994, 1995), although incurring difficulties, were able to identify by TEM major species including NaCl, sulfates, and nitrates of aerosol particles collected. Huang and Turpin (1996) discussed a method of reducing the effects of electron beam damage when determining the elemental composition of individual particles via EDS. To avoid sulfate beam damage, the sulfates were exposed to ammonia and converted to the more electron beam-stable form of ammonium sulfate.

Because of the nature of our sequential experiments, sodium chloride and sodium nitrate crystals in this study were exposed to several doses of the electron beam. The low melting point of sodium nitrate (m.p. 580 K, with decomposition at 653 K [Lide, 1991]) was of greatest concern for possible degradation. In preliminary studies, the sodium chloride crystals (m.p. 1074 K) also showed signs of severe electron beam-induced damage. These studies were undertaken to elucidate void formation and sample decomposition control measures so that TEM could be successfully used to follow the reaction of single-crystal NaCl with HNO_3 vapor followed by H_2O vapor by incorporating these decomposition control techniques. By using various techniques such as limiting exposure time, limiting electron density, and avoiding focusing directly on the sample, damage did not significantly alter the outcome of our sequential experiment. Chemical and physical reactions were monitored without significant interference from structural changes caused by the electron irradiation.

MATERIALS AND METHODS

Sodium chloride crystals were typically grown from a 0.2M NaCl solution on a Pelco carbon-coated grid (either copper or nickel). For each grid, two to three small droplets of NaCl solution were initially placed on a petri dish. Wiping of the grid over the droplets coalesced the drops underneath the Formvar and carbon coating. The grids were then allowed to "float" on top of the solution at ~ 298 K until evaporation of the solution was complete (~ 30 min). Cubic sodium chloride particles in the micrometer size range were obtained by periodic agitation during the crystallization process. The resulting crystals were utilized in the beam

damage experiments and for the reaction sequence comprised of exposure to $\text{HNO}_{3(g)}$ and $\text{H}_2\text{O}_{(g)}$.

All samples were studied using transmission electron microscopy–energy dispersive spectroscopy (TEM-EDS) at the University of California Irvine TEM facility in a Philips CM20 TEM at 200 kV with an EDAX 9800. Electron beam damage was monitored in several studies. In addition, the experiments identified changes in the morphology and composition of the sodium chloride after exposures to nitric acid and water vapor.

For the electron beam irradiation experiments, the sodium chloride crystals were exposed to varying electron densities at 200 kV with the TEM grids held at either room temperature or at ~ 120 K, cooled with a liquid nitrogen stage. For the reaction sequence experiments, NaCl crystals were exposed to nitric acid vapor as a mixture in helium inside an all-glass gas-handling manifold. Water vapor exposures were carried out by exposure either to laboratory relative humidity (RH) (during transport to and from the TEM) and/or to the vapor pressure from a reservoir of deionized water. Inside the all-glass manifold, water vapor pressure was measured by two different Edwards high vacuum pressure gauges (600AB transducer 1000 Torr range with a Model 1500 electronic manometer and a 570AB transducer 1000 Torr range with a Model 1174 electronic manometer). The manifold RH was calculated from the pressure measurements and the temperature. The relative humidity to which the sample was exposed (atmospheric water vapor) was recorded by a Fisher Scientific humidity/temperature meter (Digital Tachometer, Model #11-88-6), calibrated against the National Institute of Standards and Technology Traceable Instrumentation with a limit of error of $\pm 1.5\%$ RH and ± 0.2 K.

In order to complete a series of four experiments on the same particle with highly controlled atmospheric conditions, we chose to conduct the experiment shown in Figure 6a–d during a low RH meteorological condition (Santa Ana condition: local low RH weather phenomena that typically persists in Southern California for 2–4 days several times yearly). For reaction sequences described later in the discussion of Figure 6, the same NaCl single crystal was imaged. The electron beam was focused adjacent to the sample and a relatively low electron density was used to inhibit extensive void formation and sample decomposition. In the process of transferring the grid to and from the TEM, it was exposed to laboratory air where the RH was between 17% and 24%. The sample was then exposed to flowing nitric acid vapor outside the TEM (in a glass flow manifold), then

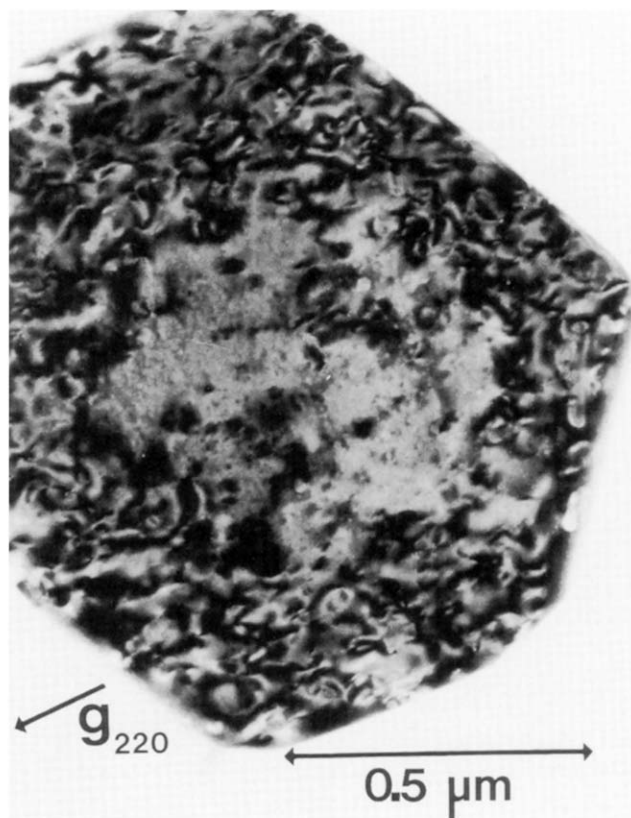


Figure 1. Micrometer-size NaCl crystal near [111] orientation showing high dislocation density after electron irradiation. Imaged using a two-beam condition. No cooling, high-electron density.

imaged. The NaCl crystals were then exposed in the glass flow manifold to a maximum RH of 71% for 2 min, then placed in the TEM. It was then reacted a second time with the same concentration of nitric acid vapor followed by a RH of 45–56%. For more details on experimental exposures, see Allen et al. (1996).

RESULTS

Figure 1 illustrates one of the results of beam damage—characteristic dislocation loops. Tilted on one of its cubic corners, this single crystal was irradiated with 200 keV (largest condenser aperture, 200 μm, and 200 nm spot size) and was imaged using a two-beam TEM condition. Electron irradiation and subsequent aggregation of point defects generated by electron radiation resulted in the density of dislocations in this crystal.

Another sample is shown in Figure 2, a 0.2-μm diameter NaCl cubic crystal with typical damage produced by the

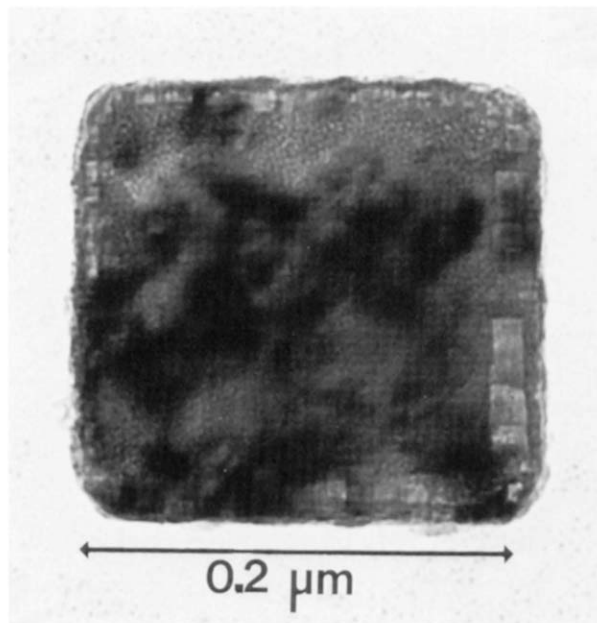


Figure 2. A 0.2- μm NaCl crystal shows severe electron beam damage and void formation. Sodium metal precipitate may have formed on the NaCl surface (most obvious in the top portion of the crystal). No cooling, high-electron density.

electron beam (largest condenser size of 200 μm , 145 nm beam spot size). In Figure 1, a high dislocation density can be resolved from the utilization of an appropriate two-beam imaging condition. Images of Figures 2–6 were not at two-beam conditions. Thus, dislocation loops are not visible in these images, although inherent saturation of defects from electron irradiation and the formation of dislocation loops are expected to have occurred. Because of the small size of the crystal in Figure 2 and the need to use a highly focused beam in order to obtain sufficient image brightness at the high magnification, this crystal showed degradation effects (i.e., void formation and possible sodium metal precipitation) within a few seconds with exposure to the electron beam. Cubic-shaped voids have formed along the crystal edges and precipitate of sodium metal may have formed (visible on the upper portion of the crystal). The smaller 0.2- μm size of this crystal shows more sensitivity to void formation even at smaller beam densities (145 nm spot size) compared with the larger NaCl crystal in Figure 1 (~ 1 μm diameter).

To minimize heating and decomposition, the TEM grid holding the NaCl crystals was held at 123 K using a liquid nitrogen cold stage and the electron density was minimized by reducing the electron beam spot size to 105 nm for Figure 3a,b (145 nm beam size was used for Figure 3c,d).

The results are presented in Figure 3a–d. TEM irradiation time between the first three images was 10 min. The fourth image was observed less than an hour after the first image. The sample was held in the electron beam for the duration. By using these two important techniques, cooling and lower electron density, this 0.4- μm sodium chloride single crystal did not show significant void formation until approximately 10 min after constant electron irradiation. This can be compared with Figure 2 in which severe void formation was observed after only a few seconds of electron irradiation.

The results of imaging larger sodium chloride single crystals at a lower magnification, but without cooling, is shown in Figure 4a and c. Severe electron beam damage occurred after a beam exposure time of 20 min (Fig. 4c). The edges of this NaCl crystal appeared to rapidly sublime and recondense in the TEM to form separate NaCl crystals (or possibly sodium metal particles) with different orientations. The diffraction pattern originally showed only a [012] single crystal pattern (Fig. 4b). After 20 min of electron bombardment there are extra diffraction spots beginning to form rings in the electron diffraction pattern (Fig. 4d), corresponding to a random orientation of NaCl or Na metal crystals. The d-spacings of fcc NaCl and fcc Na are within the measurement error and difficult to distinguish from one another.

Figure 5 shows that after NaCl is exposed to HNO_3 and water vapor, small sodium nitrate crystallites are formed on the edges of this sodium chloride host crystal (Fig. 5a). EDS analyses were acquired for chemical identification. For EDS, the electron beam was condensed in size to increase the electron density, and it was maintained over the area being analyzed until the EDS X-ray detection count was sufficient. (The time considered sufficient varies from element to element, with the lighter elements such as sodium being slower compared with chlorine because of sodium's low X-ray emission rate.) EDS did confirm the presence of Na. The small NaNO_3 crystals on the surface of the NaCl were significantly damaged during the EDS collection (Fig. 5b). The sodium nitrate crystallite in the lower right corner shows the outline of the round electron beam. Sodium nitrate decomposes readily and restructures to minimize the surface energy upon continuous electron irradiation. Electron irradiation induces local heating which then increases the mobility of the ions within the sodium nitrate lattice. The smallest NaNO_3 crystals decomposed instantaneously under electron beam exposure even though cooling techniques were employed.

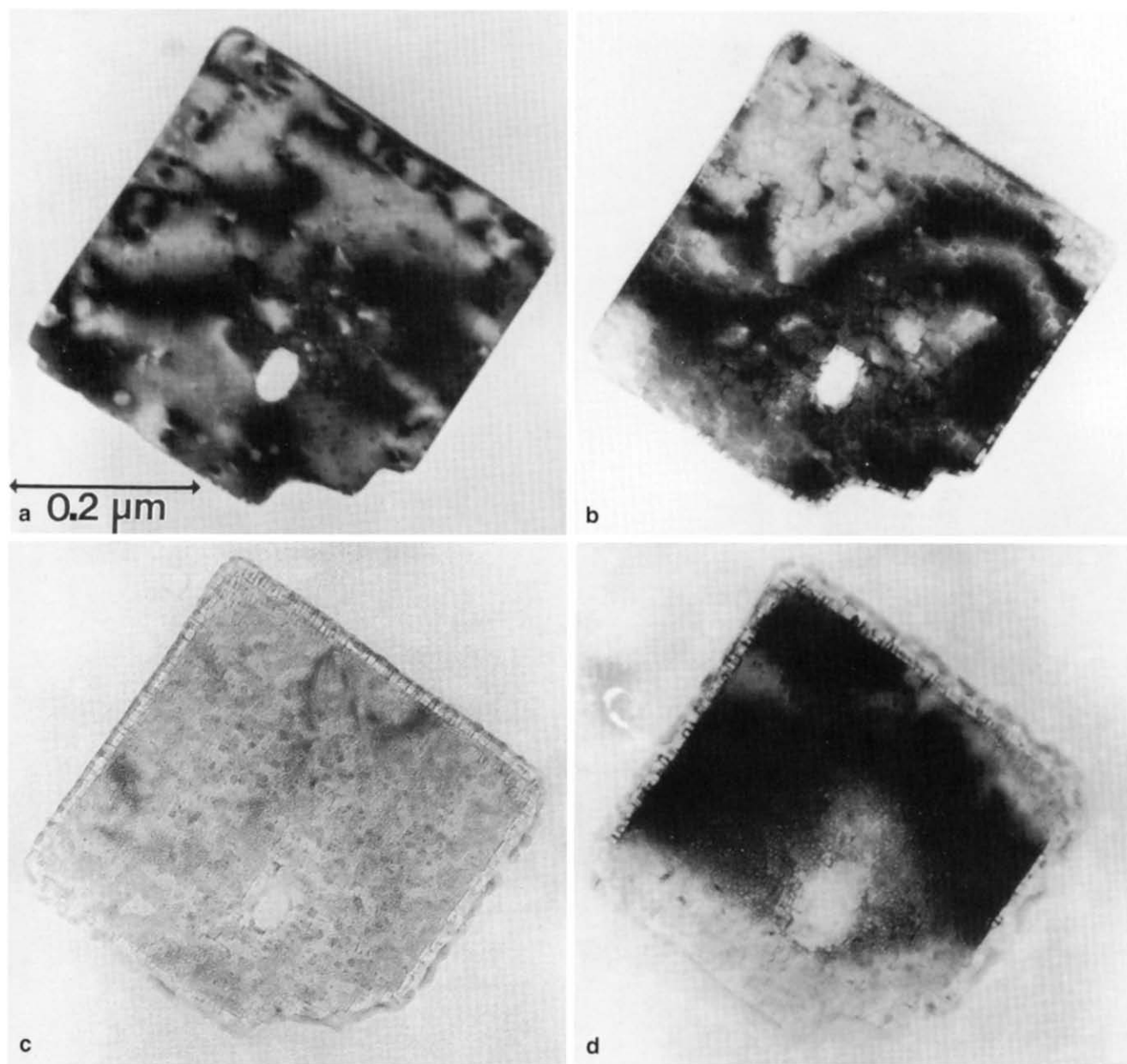


Figure 3. a: This NaCl crystal was cooled via use of a liquid nitrogen cold stage to 123 K and lens and aperture adjustments minimized electron density. **b:** After 10 min electron beam expo-

sure. **c:** After a total of 20 min electron beam exposure (lower contrast is due in part to crystal bending and deviation in tilt). **d:** After beam exposure approaching 60 min.

A modified in situ experiment using TEM was completed, where imaging the sample at reaction intervals gave a “snapshot in time” of the ongoing reaction. In the micrographs presented in Figures 6a–d, particles were successfully imaged, removed from TEM, reacted, then located again within the TEM using a combination of techniques. The sample in Figure 6 was imaged at room temperature with relatively low electron density, without extensive sample decomposition. Focusing the electron beam adja-

cent to the area of interest reduced the electron exposure time and subsequent decomposition. Figure 6a shows that crystal before any gas exposure or reaction. Figure 6b shows the same crystal after exposure to a flow of nitric acid vapor outside the TEM. The morphology has not changed in Figure 6b (compared with Fig. 6a), but after water vapor exposure, Figure 6c shows that small crystals have formed on the surface of the NaCl host crystal. Figure 6d shows that after this second cycling of HNO_3 and then H_2O vapor,

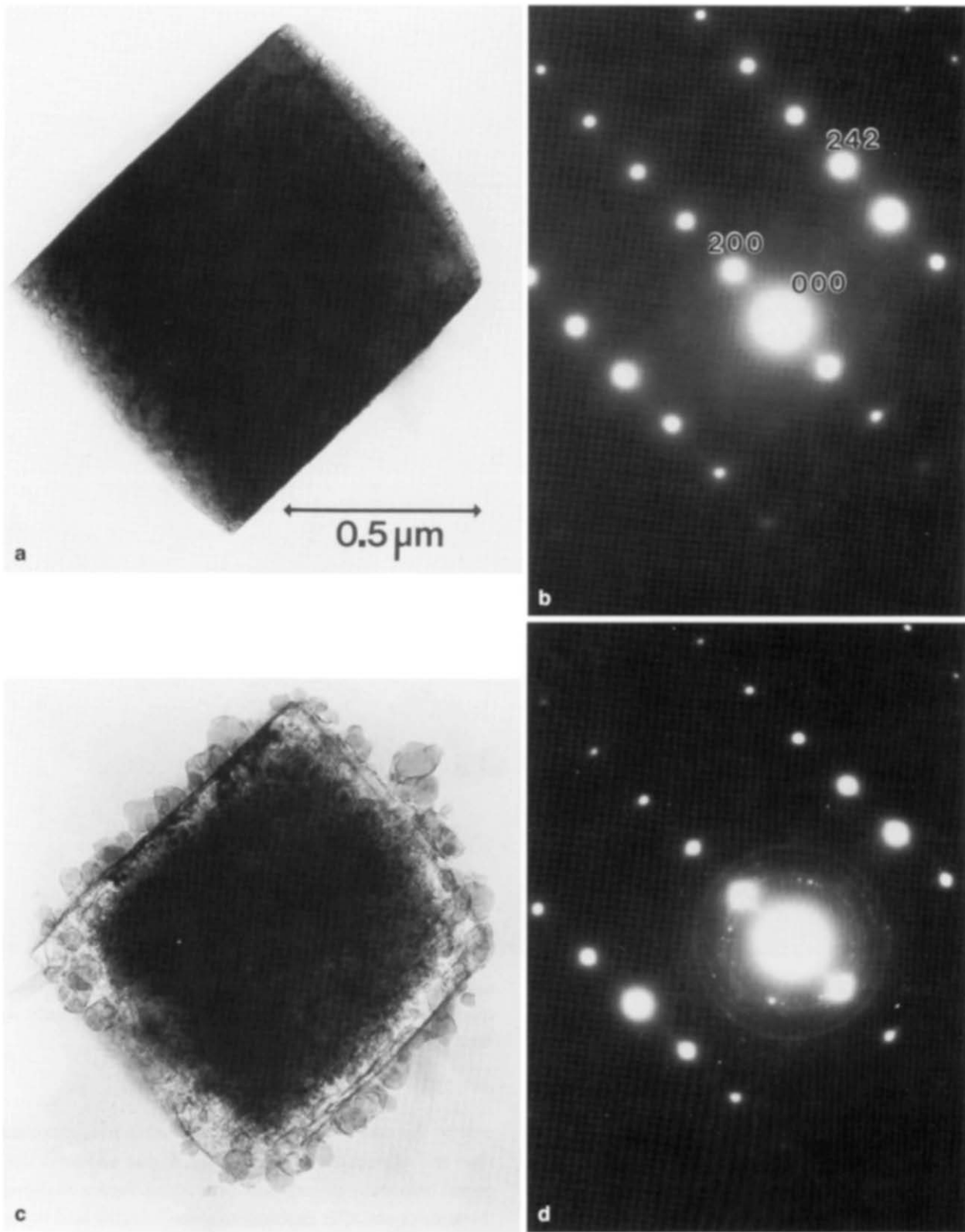


Figure 4. **a:** Larger NaCl with orientation [012]. No cooling but lower magnification was used. **b:** [012] diffraction pattern of the face-centered cubic NaCl. **c:** After exposure of 20 min. **d:** Diffraction

pattern after 20 min beam exposure. Extra spots form ring-like patterns around the transmitted beam (brightest spot) and correspond to polycrystalline NaCl or possibly Na metal.

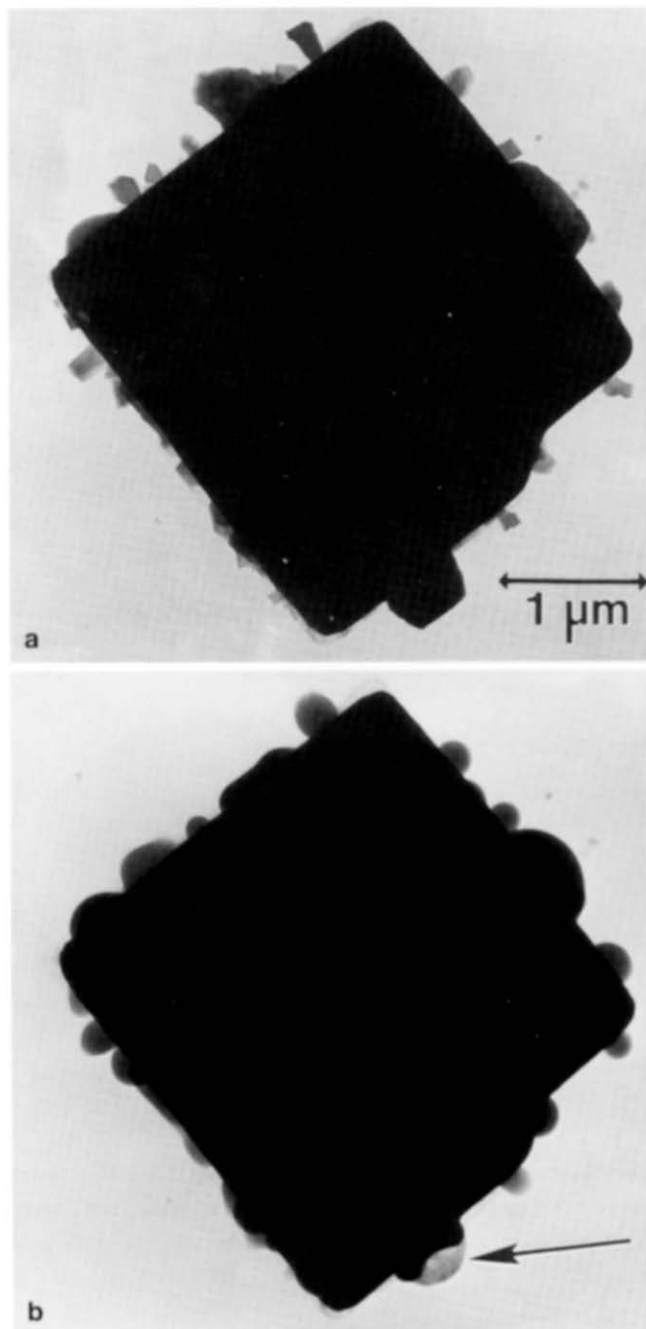


Figure 5. **a:** NaCl host crystal with NaNO_3 crystallites before EDS acquisition. **b:** After EDS acquisition using a condensed electron beam. The arrow points to a sodium nitrate crystallite that has partially sublimed and left the concave shape of the electron beam. Cooling to 102 K but high electron density used.

even smaller crystals have formed in addition to the previously formed crystals on the NaCl host crystal. The sequence of nitric acid vapor followed by water vapor exposure is critical to the formation of these small crystals on the sodium chloride host crystal. EDS spectra did confirm the lack of chlorine in the newly formed crystals.

Previously, experiments were performed and reported in which the sodium chloride crystals were not exposed to electron irradiation prior to exposure to HNO_3 vapor and H_2O vapor (Allen, 1997). TEM images taken after the chemical exposures showed the same phenomenon occurring as that presented here in the sequential experiment images (Fig. 6c,d).

DISCUSSION

Figures 1–5 demonstrate degradation effects that are caused by TEM beam exposure. These figures also demonstrate the importance of careful sample handling to reduce heating and sample decomposition. Figures 1–6 show conclusively that one can significantly reduce electron induced heating and decomposition by incorporating the following techniques: (1) focusing the beam adjacent to the sample, (2) lowering the electron density, (3) choosing to follow the reaction sequence of larger ($>1 \mu\text{m}$) NaCl crystals, and (4) lowering temperature by active cooling of the grid containment stage with liquid nitrogen. After comparison of exposure parameters for Figures 1–4, it is clear that using larger ($>1 \mu\text{m}$ NaCl) crystals, low electron density doses and cooling need to be employed in order to most effectively minimize void formation and decomposition in NaCl. To follow the reaction sequence shown in Figures 6a–6d, methods 1 through 3 were incorporated. Other experiments were successfully performed by incorporating all four techniques, but technique 4 increased the transfer time into and out of the TEM from 20 min to several hours per transfer. This is mainly due to the time it takes to warm the grid in UHV from $\sim 120 \text{ K}$ to room temperature without heating the sample prior to removing the grid from the TEM. The last step is critical so that water condensation will not occur on the grid, saturating the samples.

We present studies demonstrating the effectiveness of careful sample handling. However, damage is unavoidable, with dislocation formation being the dominant and immediate discernible form of damage. Cooling and sample handling techniques permit observation to take place while limiting the sample decomposition. This is important when following a sequential experiment such as that shown in Figure 6.

As shown in Figures 1–5, electron beam damage presents many difficulties when trying to image reactions on alkali halides such as sodium chloride (and low melting point crystalline solids such as sodium nitrate). Dislocations

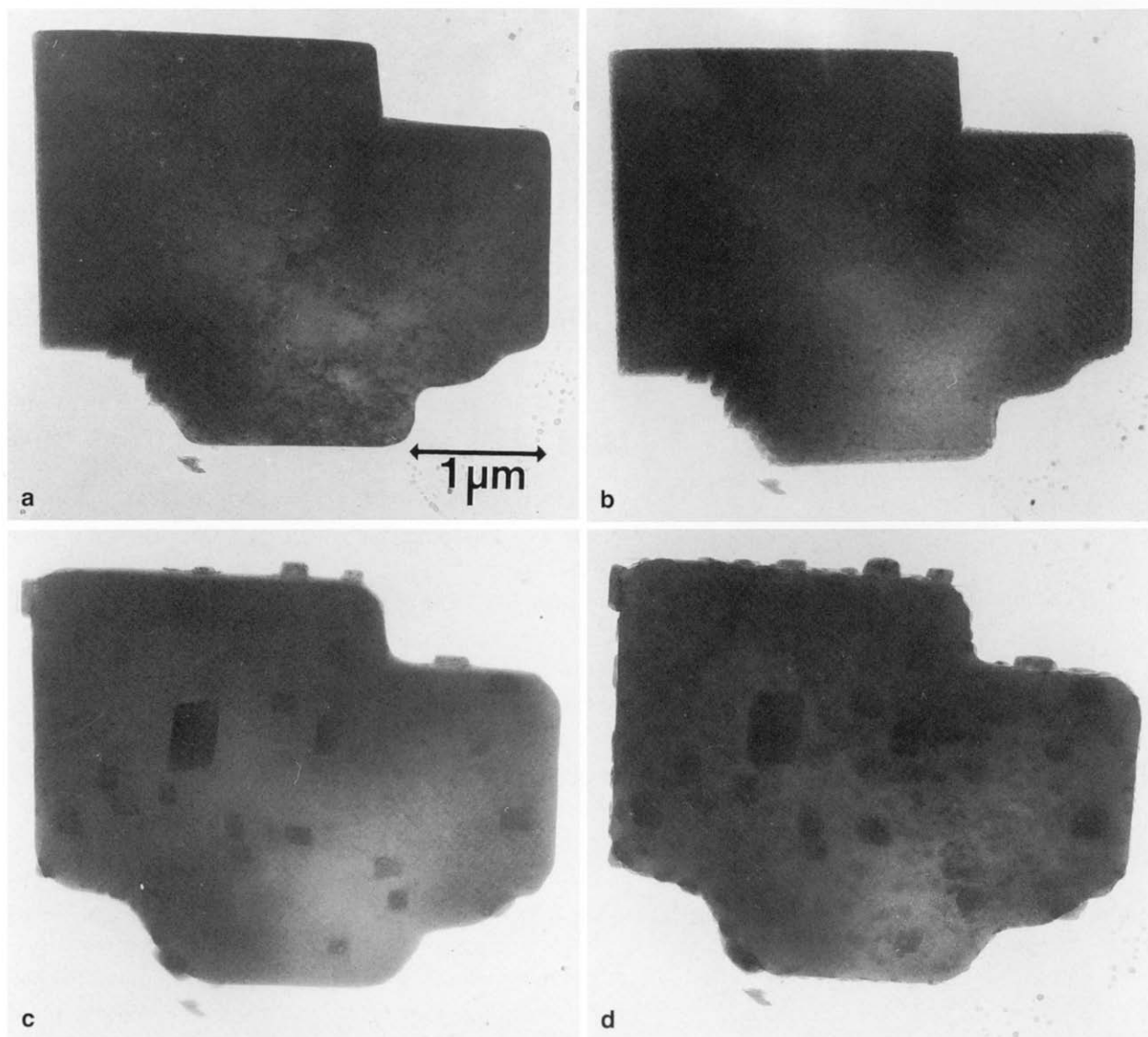


Figure 6. Successful reaction sequence using low-dose imaging. **a:** NaCl single crystal before any reaction. **b:** The same NaCl crystal after exposure to nitric acid vapor. **c:** After **b** was imaged, the NaCl crystal was exposed to 71% relative humidity. **d:** The same crystal

after another complete cycle of nitric acid vapor and then water vapor exposure (~50% RH). No cooling, but a low electron density was used, and the electron beam was focused adjacent to the area imaged.

and loop structures such as those observed in Figure 1 have been previously observed and monitored in several studies of NaCl (Hobbs et al., 1973; Hobbs, 1974; Makin, 1978; Smiser and McGee, 1969). In Figure 1, we observe a network of dislocations where some loop structures are visible. Dislocation loops are formed from the aggregation of H-centers (interstitial halogen molecules). The loops are interstitial in character and correlate with H-center mobility and density. Hobbs (1974, Fig. 34b) observed a dense dislocation network formed from repeated loop intersections on NaCl after very high electron doses, similar to that in Figure 1.

Electron beam damage of alkali halides has been well documented and the theory developed. A brief account and simplistic view of the effects of electron beam damage is presented here. For details, the reader is referred to the literature (Hobbs, 1974, 1976, 1979, 1983, 1985, 1987; and Catlow et al., 1980). Point defects occur immediately with electron irradiation. Irradiation of sodium chloride initially causes interstitials to form within the halogen sublattice. F-centers are associated with the chlorine vacancies, and H-centers with the formation of interstitial chlorine. Interstitial molecules can then form (possibly Cl_2 or Cl_3^-). Point defects will accumulate and nucleate dislocation loops. Even

at low temperatures (i.e., with liquid nitrogen cooling), the aggregation of interstitial chlorine can form gaseous halogen bubbles of Cl_2 and sample decomposition can follow by the escape of chlorine gas. The resultant voids facet on {100} planes (Hobbs, 1983, 1985; Hobbs et al., 1973). At higher sample temperatures, higher mobility of the vacancies and interstitials allows void formation to occur more readily. In addition, colloidal sodium can be produced as a byproduct from electron irradiation (Hobbs, 1974). In this case, dislocation loops serve as a sink for vacancies, allowing colloidal sodium to form.

Figures 1–5 illustrate many of the degradation effects summarized: dislocation loops (Fig. 1), formation of voids (Fig. 2) followed by sample decomposition (Figs. 2–4), and in some cases, possible sodium metal formation (Figs. 2 and 4).

In Figure 4a–d, we observed disappearance of portions of the NaCl crystal edges immediately followed by the appearance of irregularly shaped crystals. Observing the NaCl crystal edges immediately before the disappearance of the same edge areas can be compared with watching grease splatter from an extremely hot frying pan. The disappearance and reappearance of solid matter may be attributed to the sublimation of the NaCl crystal edges followed by condensation to form separate randomly oriented NaCl or Na metal crystals. Sublimation of NaCl has previously been observed in TEM (Reimer, 1989). The NaCl crystals that formed (Fig. 4c) show additional diffraction spots (Fig. 4d) in a ring-like pattern that correspond to either the fcc NaCl or fcc Na d-spacings. Previous studies by Diehl et al. (1990) have shown that alkali earth fluorides become polycrystalline with electron irradiation, and with extended electron exposure time, the diffraction spots multiply to form ring-like polycrystalline patterns.

Figure 5b illustrates the effects of localized heating. The thickness of the NaCl host crystal limits the ability to distinguish beam damage effects of this crystal. However, obvious morphology changes to the sodium nitrate crystals were observed. Even though the surrounding grid was held at temperatures of 102 K, the lower melting point crystal (sodium nitrate) decomposed. During this evaporation (and decomposition), there was no detectable temperature variation of the grid holding the crystallite. When a comparatively lower electron density was used, structural changes of the sodium nitrate crystal were observed as compared to sublimation. During EDS acquisition, a higher beam density is required and therefore one would expect increased temperatures and subsequent sublimation and/or

decomposition of sodium nitrate. This phenomenon has also been observed in atmospheric aerosol studies, where accurate quantification is affected by electron radiation effects. In one such study, sulfate samples sublimed and resulted in lower-than-expected elemental composition by EDS analysis (Huang and Turpin, 1996).

Electron-stimulated emission of NO and O_2 with relatively smaller emission of Na and NO_2 was observed by Shin and co-workers (1995) from single-crystal NaNO_3 . Emission of H^+ was also observed and was attributed to inherent hydroxylation of the nitrate groups. Sodium nitrate decomposition was shown to occur in other such studies as well (Aduru et al., 1986; Knutsen and Orlando, 1996). In agreement with these results, we also observed decomposition of the NaNO_3 . Pósfai et al. (1995) also encountered beam damage when viewing NaNO_3 particles and observed, as we did, crystals changing their surface structure to an amorphous state from exposure to higher electron density doses (Pósfai, private communication).

The sequential experiment shown in Figure 6 illustrates the successful application of TEM to obtain chemical reaction information. Beam damage has occurred; however, sample decomposition was minimized. This allowed the continued monitoring of the reaction sequence. Previously, X-ray photoelectron spectroscopy (XPS) experiments have shown that a passivating nitrate layer formed initially on the surface of NaCl single crystals after exposure to nitric acid vapor (Allen, 1996). Water vapor exposure changed the relative surface elemental composition, but there was no clear explanation for this phenomenon. An explanation consistent with the TEM studies is that water vapor exposure facilitates the reorganization of the surface. It is also important to note that similar results were obtained when NaCl crystals were exposed to nitric acid vapor and then water vapor without prior electron irradiation, proving that the reorganization of the surface is not due to electron beam damage (Allen, 1997).

SUMMARY

The formation of dislocation loops and voids was observed when studying electron beam damage effects on NaCl. However, by limiting electron beam damage in the TEM, the imaging of alkali halide reaction sequences at 200 kV is possible. The micrographs presented in this study have shown that sample decomposition that occurs from electron beam exposure can be limited by (1) focusing the beam

adjacent to the sample, (2) lowering electron density, (3) choosing to follow the reaction sequence of larger ($>1 \mu\text{m}$) NaCl crystals, and (4) lowering temperature by active cooling of the grid containment stage with liquid nitrogen. Furthermore, these studies indicate that a NaCl crystal can be successfully imaged in a series of four reaction sequences with minimal interference from sample decomposition. Using techniques 1–3, we were able to show that exposures to HNO_3 and water vapor can lead to major reconstruction and concurrent crystallization of NaNO_3 on the crystal surface. Consequently, a larger fraction of NaCl in the atmosphere is available for reaction with atmospheric pollutants. Studies conducted prior to our sequential experiment indicate that electron irradiation damage has not substantially influenced the surface chemistry. There is no passivation of the surface once the reacted sample is exposed to water vapor. Our TEM results show that the sodium chloride continually renews its surface once the NaCl surface has reacted and then has been exposed to water vapor. This reorganization phenomenon suggests that sea salt can be a significant source of atmospheric gas-phase chlorine, which may detrimentally influence ozone levels. In addition, TEM is shown to be an important complementary tool for use in studies of chemical reactions on surfaces.

ACKNOWLEDGMENTS

The authors are grateful to Professor Barbara Finlayson-Pitts for helpful comments, the National Science Foundation (Grants ATM-9302475 and ATM-9222769), the Joan Irvine Smith and Athalie R. Clarke Foundation, and the Fannie and John Hertz Foundation for their support of this work. We also thank Dr. Mehály Pósfai and Professor Peter Buseck for helpful discussions on sodium nitrate beam damage. Appreciation is also given to a reviewer for important clarification and comments on alkali halide beam damage.

REFERENCES

Aduro S, Contarini S, Rabalais JW (1986) Electron-, X-ray, and ion-stimulated decomposition of nitrate salts. *J Phys Chem* 90: 1683–1688

Allen HC (1997) Fundamental surface processes in heterogeneous atmospheric chemistry: Applications to sea-salt (NaCl) and oxide particulate chemistry. Dissertation, University of California, Irvine

Allen HC, Laux JM, Vogt R, Finlayson-Pitts BJ, Hemminger JC (1996) Water-induced reorganization of ultrathin nitrate films on NaCl: Implications for the tropospheric chemistry of sea salt particles. *J Phys Chem* 100:6371–6375

Blanchard DC (1985) The oceanic production of atmospheric sea salt. *J Geophys Res* 90:961–963

Catlow CRA, Diller KM, Hobbs LW (1980) Irradiation-induced defects in alkali halide crystals. *Phil Mag* 42:123–150

DeBock LA, VanMalderen H, VanGrieken RE (1994) Individual aerosol particle composition variations in air masses crossing the north sea. *Environ Sci Technol* 28:1513–1520

Diehl P, McCartney MR, Smith DJ (1990) Effects of electron irradiation on alkaline earth fluorides. In: *Proceedings of the XIIth International Congress for Electron Microscopy*, San Francisco: San Francisco Press, Inc., p 794

Fenter FF, Caloz F, Rossi MJ (1994) Kinetics of nitric acid uptake by salt. *J Phys Chem* 98:9801–9810

Finlayson-Pitts BJ (1983) Reaction of NO_2 with NaCl and atmospheric implications of NOCl formation. *Nature* 306:676–677

Finlayson-Pitts BJ (1993) Chlorine atoms as a potential tropospheric oxidant in the marine boundary layer. *Res Chem Int* 19: 235–249

Finlayson-Pitts BJ, Pitts JN, Jr (1986) *Atmospheric Chemistry: Fundamentals and Experimental Techniques*. New York: John Wiley and Sons

Graedel TE, Keene WC (1995) Tropospheric budget of reactive chlorine. *Global Biogeochemical Cycles* 9:47–77

Hibi T, Yada K (1962) Direct observation of crystal imperfections in KCl single crystal by electron microscope. *J Appl Phys* 33:3530–3536

Hidy GM, Mueller PK, Wang HH, Twiss KS, Imada M, Alcocer A (1974) Observations of aerosols over southern California coastal waters. *J Appl Meteorol* 13:96–107

Hobbs LW (1974) Transmission electron microscopy of extended defects in alkali halide crystals. In: *Surface and Defect Properties of Solids*, vol. 4. London: The Chemical Society, pp 153–250

Hobbs LW (1976) Point defect stabilization in ionic crystals at high defect concentrations. *J Phys* 37:C7-3–C7-26

Hobbs LW (1979) Radiation effects in analysis of inorganic specimens by TEM. In: *Introduction to Analytical Electron Microscopy*. New York: Plenum Press, pp 437–480

Hobbs LW (1983) Radiation effects in analysis by TEM. In: *Quantitative Electron Microscopy Proceedings of the Twenty Fifth Scottish*

- Universities Summer School in Physics, Glasgow, Scotland: Scottish Universities Summer School in Physics, pp 399–445
- Hobbs L (1985) Radiation effects in the electron microscope. *EMSA Bull* 15:51–63
- Hobbs LW (1987) Electron-beam sensitivity in inorganic specimens. *Ultramicroscopy* 23:339–344
- Hobbs LW, Hughes AE, Pooley D (1973) A study of interstitial clusters in irradiated alkali halides using direct electron microscopy. *Proc R Soc Lond A* 332:157–185
- Huang P, Turpin B (1996) Reduction of sampling and analytical errors for electron microscopic analysis of atmospheric aerosols. *Atmospheric Environ* 30:4137–4148
- Karlsson R, Ljungstrom E (1995) Nitrogen dioxide and sea salt particles—a laboratory study. *J Aerosol Sci* 26:39–50
- Knutsen K, Orlando TM (1996) Low energy (5–80 eV) electron-stimulated desorption of H^+ (D^+), OH^+ (OD^+), O^+ , and NO^+ from solution-grown $NaNO_3$ crystals. *Surf Sci* 348:143–152
- Laux JM, Hemminger JC, Finlayson-Pitts BJ (1994) X-ray photoelectron spectroscopic studies of the heterogeneous reaction of gaseous nitric acid with sodium chloride: Kinetics and contribution to the chemistry of the marine troposphere. *Geophys Res Lett* 21:1623–1626
- Laux JM, Fister TF, Hemminger JC, Finlayson-Pitts BJ (1996) X-ray photoelectron spectroscopy studies of the effects of water vapor on ultra-thin nitrate layers on NaCl. *J Phys Chem* 100:19891–19897
- Leu MT, Timonen RS, Keyser LF, Yung YL (1995) $HNO_{3(g)} + NaCl_{(s)} \rightarrow HCl_{(g)} + NaNO_{3(g)}$ and $N_2O_{5(g)} + NaCl_{(s)} \rightarrow ClNO_{2(g)} + NaNO_{3(s)}$. *J Phys Chem* 99:13203–13212
- Lide DR, ed (1991) *CRC Handbook of Chemistry and Physics 1991–1992*, Boca Raton, FL: CRC Press, section 4, pp 98–99
- Makin MJ (1978) Atom displacement radiation damage in electron microscopes. In: *Ninth International Congress on Electron Microscopy*, III, Toronto, pp 330–342
- Martens CS, Wesolowski JJ, Harriss RC, Kaifer R (1973) Chlorine loss from Puerto Rican and San Francisco bay area marine aerosols. *J Geophys Res* 78:8778–8792
- Pósfai M, Anderson JR, Buseck PR, Shattuck TW, Tindale NW (1994) Constituents of a remote pacific marine aerosol: A TEM study. *Atmospher Environ* 28:1747–1756
- Pósfai M, Anderson JR, Buseck PR, Sievering H (1995) Compositional variations of sea-salt-mode aerosol particles from the North Atlantic. *J Geophys Res* 100:23063–23074
- Reimer L (1989) *Springer Series in Optical Sciences: Transmission Electron Microscopy, Physics of Image Formation and Microanalysis* 2nd ed. New York: Springer-Verlag
- Shaw GE (1991) Aerosol chemical components in Alaska air masses 2. Sea salt and marine product. *J Geophys Res* 96:22369–22372
- Sheridan PJ, Schnell RC, Hofmann DJ, Harris JM, Deshler T (1992) Electron microscope studies of aerosol layers with likely Kuwaiti origins over Laramie, Wyoming during spring 1991. *Geophys Res Lett* 19:389–392
- Shin JJ, Langford SC, Dickinson JT, Wu Y (1995) Electron stimulated neutral and ion emission from single crystal $NaNO_3$. *Nucl Instruments Methods Phys Res B* 103:284–296
- Smiser LW, McGee TD (1969) Transmission electron microscopy of sodium chloride. *J Am Ceramic Soc* 52:681–682
- Vogt R, Finlayson-Pitts BJ (1994a) Tropospheric HONO and reactions of oxides of nitrogen with NaCl. *Geophys Res Lett* 21:2291–2294
- Vogt R, Finlayson-Pitts BJ (1994b) A diffuse reflectance infrared fourier Transform spectroscopic (DRIFTS) study of the surface reaction of NaCl with gaseous NO_2 and HNO_3 . *J Phys Chem* 98:3747–3755; 99:13052
- Xhoffer C, Bernard P, VanGrieken R (1991) Chemical characterization and source apportionment of individual aerosol particles over the north sea and the English Channel using multivariate techniques. *Environ Sci Technol* 25:1470–1478